

図3 長期フォローアップセンターのイメージ

治療終了時にサマリーを作成し、リスク因子に応じた長期FU計画を立て、治療施設と患児・家族に送付する。その計画に従い、最初の数年間は治療施設で、その後は長期FU拠点病院を主体として、晩期障害を中心としたFUを行う。問題が生じた場合はセンターと連絡を取りながら、晩期障害に対する早期対応を行う。また、これらのデータはすべてセンターに蓄積される。長期FUセンターに登録した小児がん経験者は、一生の間日本中どこにいても、インターネット等で自分の蓄積された情報にアクセスでき、自分自身の健康管理に活用できる。

(藤本原図より改変)

きる医療へと移行することについて、長期FU移行プログラムが必要となる。大人になろうとしている彼等に必要な医療的ケアは、技術的に小児医療の枠を超えたものであることを明確に説明し、小児がん経験者として、スムーズな次段階への移行が重要であることの理解を求め、移行の過程を無事、経過できるよう手助けすることが、小児がん経験者の自立心を生み出す結果につながると考えられる²⁾。今後小児科医は患者離れを上手に行いながらも、常に様々な問題の相談者として小児がん経験者を陰ながら支えるという姿勢が大切と思われる。

3. JPLSG 長期FU委員会の取り組み

現在の長期FU委員会活動としては、(1)長期FU外来を可能な施設で設置してもらうための働

きかけ、(2)治療総括サマリーの全国標準化の推進、(3)晩期障害別の情報整理として、小児がんの晩期障害に関する成書 (Schwartz CL et al 「Survivors of Childhood and Adolescent Cancer」²⁾) の翻訳・監訳作業、(4)シンポジウム・パネルディスカッションの開催 (小児内分泌学会の小児がんサバイバーのための委員会との連絡、産婦人科医師との連携、小児がん経験者や家族を対象に情報交換)、(5)他の治療研究グループ (JPLSG 以外の小児がん固形腫瘍研究グループ) との調整・共同などである。

最後に、JPLSG 長期FU委員会で検討中の長期FUシステム案を紹介する (図3)。治療終了時には長期FUに関する同意書を取得し、実名登録後その患児の治療内容を総括して今後のFU計画を立てる。長期FUセンターには個人情報を含めたFUデータが集積され、登録した小児がん経験者

は一生の間、日本中どこにいてもインターネットなどの手段で自分個人の集積された情報にアクセスでき、自分自身の健康管理に活用できる。また、年に1回はセンターから登録者に連絡を取り、アンケート調査を実施するとともに問題の有無を調査する。センターでは晩期障害に関する相談を電話、メール、FAX、手紙などで受け付けて、適切な地域の医療機関を紹介したり、直接相談にのる。また、センターには小児がんの晩期障害に関する世界中の最新情報を収集・蓄積し、医療者向け・患者向けに整理して、図書館やホームページから入手可能とする。センターは全国各地の長期FU可能な拠点病院とネットワークを作り、定期的なミーティングを開き情報交換を行う。また、小児がんの晩期障害に関する教育的なセミナーや講座を定期的に主催し、若い医師だけでなく看護師、臨床心理士、ソーシャルワーカーなど、コメディカル養成の場所となる。将来的には長期FUデータを集積・分析してコホート研究を行い^{17,18)}、治療研究プロトコルの問題点を明らかにして、晩期障害の少ないQOLのよい治療プロトコルの開発に寄与することを最終的な目標としていきたい。

おわりに

今後、小児がん専門家、コメディカル、小児がん経験者、その家族などと協議を重ねつつ、望ましい長期FUシステムについて議論を深めていく予定であるが、平成18年度からは次のような研究班が小児がん長期FUに関連した活動を行っている。

1. 厚生労働科学研究費補助金 (がん臨床研究事業) (班長：堀部敬三)

課題は「小児造血器腫瘍の標準的治療法の確立に関する研究」であり、堀部班がバックアップするJPLSGで、2005年4月に長期FU委員会を組

織し、JPLSG治療研究に登録された患児の晩期障害について長期FUを目標とした研究計画とシステム作りを始めた。今後はこの委員会で小児血液がんの治療終了後の長期FUが可能となる基盤整備を行い、QOL・治療法の改善のために役立つ。

2. 厚生労働省がん助成金 (班長：岡村 純)

課題は「小児がん克服者のQOLと予後の把握及びその追跡システムの確立に関する研究班」であり、臨床的な側面からレトロスペクティブな実態調査を中心に活動する。アンケート調査 (身体的/心理的晩期障害、QOL、就職/結婚/保険)、長期FUが途絶える理由等を調査中である。

3. 成育委託費 (班長：藤本純一郎)

課題は「小児がんの長期フォローアップ体制整備に関する研究」であり、患者情報の収集・保存・利用のシステム作りとハード面の検討が中心である。実名ありの個人情報はどう扱うか、小児がん登録の見直しと再構築も大きな課題であり、長期FUの拠点病院の提案も検討中である。主に欧米のシステムを参考に情報を調査するが、JPLSGと連携し、将来的にはコホート研究も検討する。

最後に、現在ではインターネットを通じて、欧米の小児がん長期FUのガイドラインが入手可能であり、内容も非常に詳細で有用なため、適宜最新版をダウンロードして参照することをおすすめしたい。

COG Long-Term Follow-Up Guidelines
(<http://www.survivorshipguidelines.org/>)

The Scottish Intercollegiate Guidelines
(<http://www.sign.ac.uk/index.html>)

NCI PDQ
(<http://jncicancerspectrum.oupjournals.org/databases/pdq/treatment.dtl>)

The Childhood Cancer Survivor Study (CCSS)
(<http://www.cancer.umn.edu/ltfu>)

本研究は、平成17・18年度厚生労働科学研究

費補助金(がん臨床研究事業)「小児造血器腫瘍の標準的治療法の確立に関する研究」、がんの子供を守る会平成17年度小児がん助成「小児がん長期フォローアップガイドラインの作成」、平成18年度厚生労働省がん助成金「小児がん克服者のQOLと予後の把握及びその追跡システムの確立に関する研究班」および平成18年度成育委託費「小児がんの長期フォローアップ体制整備に関する研究」の補助を受けた。

文 献

- 1) Wallace H, Green D: Late Effects of Childhood Cancer. London Arnold, 2004
- 2) Schwartz C, Hobbie W, Constine L, Ruccione K: Survivors of Childhood and Adolescent Cancer. Berlin, Springer-Verlag, 2005 (現在翻訳中)
- 3) 石田也寸志: 北米 Childhood Cancer Survivor Study による小児がん経験者の長期的な問題点—第1編. 日本小児科学会雑誌 **110**: 1513, 2006
- 4) 石田也寸志: 北米 Childhood Cancer Survivor Study による小児がん経験者の長期的な問題点—第2編. 日本小児科学会雑誌 **110**: 1523, 2006
- 5) 大園秀一ほか: 小児がん長期フォローアップ調査報告. 日本小児科学会雑誌 (投稿中)
- 6) Oeffinger KC, et al: Grading of late effects in young adult survivors of childhood cancer followed in an ambulatory adult setting. *Cancer* **88**: 1687-1695, 2000
- 7) Oeffinger KC, et al: Chronic health conditions in adult survivors of childhood cancer. *N Engl J Med* **355**: 1572, 2006
- 8) 石田也寸志: 小児血液疾患の合併症とその対策・白血病晩期障害, 神経障害. *小児内科* **37**: 1234, 2005
- 9) Campbell LK, et al: A meta-analysis of the neurocognitive sequelae of treatment for childhood acute lymphocytic leukemia. *Pediatr Blood Cancer*. (preview edition 2006)
- 10) Smibert E, et al: Exercise echocardiography reflects cumulative anthracycline exposure during childhood. *Pediatr Blood Cancer* **42**: 556, 2004
- 11) Van Dalen E, et al: Anthracycline-induced cardiotoxicity: Comparison of recommendations for monitoring cardiac function during therapy in paediatric oncology trials. *Eur J Cancer*.
- 12) Green DM, et al: Pregnancy outcome of female survivors of childhood cancer: a report from the Childhood Cancer Survivor Study. *Am J Obstet Gynecol* **187**: 1070, 2002
- 13) Green DM, et al: Pregnancy outcome of partners of male survivors of childhood cancer: a report from the Childhood Cancer Survivor Study. *J Clin Oncol* **21**: 716, 2003
- 14) Socie G, et al: Nonmalignant late effects after allogeneic stem cell transplantation. *Blood* **101**: 3373, 2003
- 15) Pui CH, et al: Extended follow-up of long-term survivors of childhood acute lymphoblastic leukemia. *N Engl J Med* **349**: 640, 2003
- 16) Zebrack BJ, et al: Health care for childhood cancer survivors. Insights and perspectives from a Delphi panel of young adult survivors of childhood cancer. *Cancer* **100**: 843, 2004
- 17) Robison LL, et al: Study design and cohort characteristics of the Childhood Cancer Survivor Study: a multi-institutional collaborative project. *Med Pediatr Oncol* **38**: 229, 2002
- 18) Langer T, Henze G and Beck JD: Basic methods and the developing structure of a late effects surveillance system (LESS) in the long term follow-up of pediatric cancer patients in Germany. *Med Ped Oncol* **34**: 348, 2000

Clonotypic analysis of T cell reconstitution after haematopoietic stem cell transplantation (HSCT) in patients with severe combined immunodeficiency

H. Okamoto,* C. Aii,[†] F. Shibata,*
T. Toma,* T. Wada,* M. Inoue,*
Y. Tone,* Y. Kasahara,* S. Koizumi,*
Y. Kamachi,[‡] Y. Ishida,[§] J. Inagaki,[¶]
M. Kato,** T. Morio^{††} and A. Yachie[†]

*Department of Pediatrics, Graduate School of Medical Science, Kanazawa University,

[†]Department of Clinical Laboratory Science, Division of Health Sciences, Graduate School of Medical Science, Kanazawa University,

[‡]Department of Pediatrics, Nagoya University,

[§]Department of Pediatrics, Ehime University,

[¶]Department of Pediatrics, Nara Medical University, **Gunma Children's Medical Centre,

and ^{††}Department of Pediatrics and Developmental Biology, Tokyo Dental and Medical University, Tokyo, Japan

Accepted for publication 20 February 2007

Correspondence: Akihiro Yachie MD, PhD, Department of Clinical Laboratory Science, Division of Health Sciences, Graduate School of Medical Science, Kanazawa University, 5-11-80 Kodatsuno, Kanazawa 920-0942, Japan.

E-mail: yachie@med.kanazawa-u.ac.jp

Introduction

Haematopoietic stem cell transplantation (HSCT) is the treatment of choice for various haematological malignancies. Eradication of malignant cells is achieved by intense chemotherapy performed prior to HSCT, but post-transplantation is crucial to reconstitute a functional haematological system to permit development of donor stem cells. In particular, reconstitution of a potent immune system with a diverse repertoire of T cells is of critical importance for defence against infections and tolerance induction after HSCT [1]. HSCT is now performed not only for malignant disorders but also for various autoimmune disorders [2,3] and primary immunodeficiency diseases [4–6]. In such cases, failure of effective immune reconstitution increases the risk of infections and unfavourable complications, and thereby adds to the risk of recurrence of the original disease. Therefore, monitoring the status of T cell reconstitution and use of this information in treatment is important for successful HSCT.

Summary

Haematopoietic stem cell transplantation (HSCT) is performed for treatment of a broad spectrum of illnesses. Reconstitution of an intact immune system is crucial after transplantation to avoid infectious complications, and above all, the establishment of T cell receptor (TCR) diversity is the most important goal in the procedure. Until recently, little has been known of the mechanism of T cell reconstitution in the very early period after HSCT. In this study, we analysed TCR repertoires sequentially in four patients with severe combined immunodeficiency (SCID) before and after HSCT. In all patients, the TCR repertoires were extremely abnormal before HSCT, whereas after transplantation there was progressive improvement in TCR diversity, based on analysis of the TCR V β repertoire and CDR3 size distributions. Somewhat unexpectedly, there was a significant but transient expansion of TCR diversity 1 month after transplantation in all cases. Clonotypic analysis of TCRs performed in one case showed that many T cell clones shared identical CDR3 sequences at 1 month and that the shared fraction decreased progressively. These results indicate that early expansion of TCR diversity may reflect transient expansion of pre-existing mature T cells from the donor blood, independent of *de novo* T cell maturation through the thymus.

Keywords: SCID, HSCT, T cell reconstitution, TCR diversity

Two distinct pathways of T cell reconstitution, thymus-dependent and thymus-independent, are thought to operate after HSCT [7,8]. Although T cell reconstitution through the thymus-dependent pathway first appears as early as 2 months after HSCT, it gradually increases in size and diversity over 1–2 years [7,9–11]. Quantitative recognition of the naive T cell population is usually possible 5 or 6 months after the procedure; the slow recovery of T cell numbers reflects the passage of T cells through thymic selection for discrimination between self and non-self antigens [7,12,13]. As Borghans *et al.* reported recently, successful long-term reconstitution depends on the quantity of this thymic output [14]. On the other hand, very rapid T cell reconstitution is observed in some cases, suggesting that thymus-independent expansion of donor-derived mature T cells can also occur [15–17]. These T cells, although limited in diversity, may contribute significantly to immune reconstitution very early after HSCT, at a time when thymus-derived T cells are unavailable.

Table 1. Clinical profiles and treatment characteristics of the patients.

Patient	1	2	3	4
Diagnosis	Omenn syndrome	Atypical Omenn syndrome	T-B-SCID (with MFT)	Omenn syndrome
Clinical manifestation	Eczema, diarrhoea failure to thrive Hepatosplenomegaly Lymph node swelling	Bronchitis Acute otitis media	Bronchitis <i>Carinii pneumonia</i>	Eczema Acute otitis media Hepatosplenomegaly
Mutation	RAG2	RAG1	Artemis	RAG1
Age at diagnosis	0 m	10 m	6 m	3 m
Age at HSCT	4 m	13 m	8 m	7 m
Graft	UCB 29 × 10 ⁷ /kg	UCB 3.5 × 10 ⁷ /kg	Father's BM 6.1 × 10 ⁸ /kg	UCB 5.29 × 10 ⁷ /kg
Conditioning	Flu + Bu + ATG	Flu + Cy + TBI	Flu + Bu	Flu + LPAM + ATG
GVHD prophylaxis	CyA	FK506 + sMTX	FK506 + sMTX	CyA + mPSL
GVHD (treatment)	None	Skin grade IV (mPSL + MMF)	Skin grade II Gut grade III (mPSL + MTX)	Skin grade II
Complication	None	MRSA sepsis	None	<i>Mycobacterium avium</i> Complex infection

UCB: umbilical cord blood; MFT: maternal fetal transfusion; GVHD: graft-versus-host disease; HSCT: haematopoietic stem cell transplantation.

In this study, we analysed T cell receptor (TCR) diversity sequentially before and after HSCT in four patients with severe combined immunodeficiency disorders. Detailed analysis of TCR diversity and clonotypes showed that a brief period of transient but relatively diverse T cell expansion occurs soon after HSCT in SCID patients.

Methods

Patient characteristics

The clinical characteristics and conditioning regimens for HSCT in four SCID infants are shown in Table 1. Patients 1, 2 and 4 had Omenn syndrome and related disorders with RAG1/RAG2 gene mutations. Patient 1 had heterozygous mutations in both alleles of the RAG2 gene and exhibited typical clinical manifestations. Patient 2 was atypical, in that neither peripheral eosinophilia nor expansion of activated T cells was prominent; furthermore, typical skin lesions were also absent, but a prolonged lower respiratory tract infection led to the correct diagnosis. Patient 3 had mutations in the *Artemis* gene, and *Pneumocystitis carinii* infection was found in this patient. Patient 4 had homozygous mutations in RAG1 that resulted in a frameshift and elimination of functional enzyme activity. However, multiple second-site mutations in oligoclonal T cells caused Omenn syndrome-like clinical manifestations [18]. Three patients received cord blood stem cell transplantation (CBSCT) and one patient received a haplo-identical bone marrow transplant (BMT) from his father. All these grafts were unmanipulated and were not devoid of mature T cells. All patients received non-myeloablative conditioning before transplantation; however, despite prophylaxis for

graft-versus-host disease (GVHD), three patients developed GVHD and one of these patients received methylprednisolone and mycophenolate mofetil (MMF). Approval for the study was obtained from the Human Research Committee of Kanazawa University Graduate School of Medical Science, and informed consent was obtained according to the Declaration of Helsinki.

Flow cytometry

Surface antigens expressed on lymphocytes were analysed by flow cytometry. After red blood cell (RBC) lysis and washing in phosphate-buffered saline (PBS), peripheral blood samples were incubated with monoclonal antibodies for 15 min on ice. Phycoerythrin (PE)-conjugated anti-CD3 and anti-CD20 antibodies were obtained from BD Pharmingen (San Diego, CA, USA), and PE-conjugated anti-CD4 and anti-CD8 antibodies were products of Dako (Glostrup, Denmark). Fluorescein isothiocyanate (FITC)-conjugated anti-CD16 antibody was purchased from Immunotech (Marseille, France) and FITC-conjugated anti-CD45RO antibody was obtained from Dako. After washing twice in PBS, cells were analysed with a flow cytometer [fluorescence activated cell sorter (FACSCalibur); Becton Dickinson, San Diego, CA, USA]. The resulting data were analysed using CELLQUEST software (Becton Dickinson).

The T cell receptor (TCR) Vβ repertoire distribution was analysed using three-colour flow cytometry. After RBC lysis and washing in PBS, samples were incubated with appropriate PE-conjugated monoclonal antibodies with specificity for TCR Vβ (Immunotech) for 30 min on ice, followed by FITC-conjugated anti-CD8 antibody (Becton Dickinson) and R-phycoerythrin-Cy5-conjugated anti-CD4 antibody

(Dako) for 15 min. After washing in PBS, three-colour analysis was performed with the FACSCalibur instrument.

Total RNA extraction and reverse transcription–polymerase chain reaction (RT–PCR)

Total RNA was extracted as described previously with a slight modification [19]. Briefly, peripheral blood mononuclear cells (PBMCs) were separated from heparinized peripheral blood by Ficoll–Hypaque density centrifugation. T cells were separated from PBMCs by the E-rosette method. CD4⁺ and CD8⁺ T cells were purified from T cells by negative selection using anti-CD8 or anti-CD4 magnetic beads (DynaL ASA, Oslo, Norway) [20]. The fraction of contaminating CD4⁺ T cells within the CD4-depleted cells or CD8⁺ T cells within the CD8-depleted cells was always less than 1% after the negative selection procedure. Total cellular RNA was isolated with Trizol reagent following the manufacturer's instructions (GIBCO BRL, Bethesda, MD, USA). The RNA was reverse-transcribed into cDNA in a reaction containing RandomHex Primer (TaKaRa, Otsu, Japan) and RAV-2 (TaKaRa). The concentration of RNA was measured using a GeneQuant pro RNA/DNA Calculator (Amersham Pharmacia Biotech, Cambridge, UK).

CDR3 size analysis

CDR3 spectratyping was performed as described previously [20]. Briefly, cDNA was PCR-amplified through 35 cycles (94°C for 1 min, 55°C for 1 min and 72°C for 1 min) with a primer specific to 24 different V β subfamilies (V β s 1–20 and V β s 21–24) and a fluorescent C β primer. The fluorescent PCR products were mixed with formamide and a size standard (GeneScan-500 Tamra, Applied Biosystems, Foster City, CA, USA). After denaturation for 2 min at 90°C, the products were analysed with an automated 310 DNA sequencer and GeneScan software (Applied Biosystems). The overall complexity within a V β subfamily was determined by counting the number of discrete peaks and determining their relative size on the spectratype histogram, as described previously [21]. In this analysis, the complexity score = (sum of all peak heights/sum of major peak heights) \times (number of major peaks); major peaks were defined as those peaks on the spectratype histogram with an amplitude of at least 10% of the sum of all peak heights. Numbers of undetectable V β subfamilies and mean complexity scores for detectable V β subfamily were calculated. The mean complexity scores ranged from 4.9 to 5.2 in healthy adult controls, as reported previously [22].

TCR CDR3 cloning and sequence

PCR products of selected V β cDNA were electrophoresed on an agarose gel and purified using a QIAquick Gel Extraction Kit (Qiagen, Tokyo, Japan), followed by cloning with a Topo

TA Cloning Kit (Invitrogen, Carlsbad, CA, USA). Colonies containing the insert fragment were selected randomly. After purification with a QIAprep Spin Miniprep Kit (Qiagen) the recombinant plasmids were subjected to fluorescence dye terminator cycle sequencing, and the sequence reactions were analysed on a 3100 DNA sequencer (Applied Biosystems) after removal of unincorporated fluorescence dye using a Centri-Sep Spin Column (Applied Biosystems).

Three-dimensional graphic display of TCR diversity through combination of CDR3 size analysis and V β repertoire distribution

Qualitative alterations of TCR V β repertoires obtained by CDR3 spectratyping were combined with the quantity of specific V β ⁺ CD4⁺ and CD8⁺ T cells for each V β subfamily and plotted as landscape columns, as described previously [23].

Results

Lymphocyte subset

CD3⁺ T cells constituted the majority of lymphocyte populations prior to transplantation in patients 1 and 4, who both showed typical symptoms of Omenn syndrome (Table 2). In both cases, virtually all CD4⁺ T cells and CD8⁺ T cells expressed CD45RO⁺ memory phenotypes. In contrast, the numbers of CD3⁺ T cells were low compared to the numbers of lymphocytes in patients 2 and 3; in patient 3 the detectable T cells prior to transplantation were of maternal origin, as determined by microsatellite polymorphism analysis (data not shown). Most CD4⁺ T cells expressed CD45RO, whereas CD45RO expression on CD8⁺ T cells remained relatively low in these patients. Although CD4⁺ T cells increased progressively after HSCT in all cases, recovery of CD8⁺ T cells was delayed, especially in patient 2, who suffered severe GVHD. In each case, CD45RO⁺ T cells were predominant in the early stage after transplantation, whereas CD45RO⁻ T cells started to increase 9 months after transplantation.

TCR V β repertoire distributions

Before transplantation, TCRV β repertoires were restricted in both the CD4⁺ and CD8⁺ T cell populations in all patients (Fig. 1a,b, respectively). Oligoclonal T cell expansions were particularly prominent in patients 1 and 4, who showed typical symptoms of Omenn syndrome. After HSCT the TCRV β repertoire distributions became diverse in all patients, and CD4⁺ T cells maintained the diversity of the TCRV β repertoire until 9 months after transplantation. In contrast, CD8⁺ T cells showed evidence of oligoclonal expansion of limited clones: V β 6⁺ and V β 14⁺ cells in patient 2, V β 6⁺ cells in patient 3 and V β 8⁺ and V β 12⁺ cells in patient 4 had all increased significantly at 4 months. However, the

Table 2. Changes in lymphocyte subpopulations.

Patient	Subset	Pre	1 m	4 m	9 m
1	WBC	4 100	13 400	6 400	9 200
	Lymph	1 262	670	2 611	5 336
	CD3	1 079	369	n.d.	3 431
	CD4	721	320	n.d.	2 423
	CD45RO ⁺ /CD4 (%)	97.7	84.9	n.d.	8.7
	CD8	345	46	n.d.	662
	CD45RO ⁺ /CD8 (%)	93.0	42.5	n.d.	2.6
	CD16	92	301	n.d.	678
	CD20	0	0	n.d.	1 233
2	WBC	2 800	9 800	16 000	6 900
	Lymph	1 300	1 800	2 000	1 800
	CD3	334	1 015	1 786	1 336
	CD4	289	749	1 732	1 219
	CD45RO ⁺ /CD4 (%)	97.1	79.7	98.5	71.7
	CD8	46	202	86	115
	CD45RO ⁺ /CD8 (%)	44.4	51.8	64.1	56.2
	CD16	965	718	110	328
	CD20	1	2	104	137
3	WBC	3 200	7 400	4 600	10 600
	Lymph	512	1 110	1 242	2 600
	CD3	73	931	1 098	2 428
	CD4	67	380	452	991
	CD45RO ⁺ /CD4 (%)	88.8	59.8	68.5	31.5
	CD8	14	520	653	1 446
	CD45RO ⁺ /CD8 (%)	5.9	34.9	38.5	19.6
	CD16	440	178	139	122
	CD20	0	1	1	10
4	WBC	26 600	8 100	7 500	10 000
	Lymph	19 600	400	1 020	6 300
	CD3	18 855	111	755	3 780
	CD4	9 114	84	609	2 905
	CD45RO ⁺ /CD4 (%)	99.8	70.2	91.5	15.9
	CD8	10 251	27	86	870
	CD45RO ⁺ /CD8 (%)	99.8	72.5	71.8	2.8
	CD16	725	289	95	485
	CD20	20	0	171	2 035

WBC: white blood cells; n.d.: not done. All lymphocyte numbers represent absolute numbers/ μ l. CD45RO (%) shows percentages of CD45RO⁺ cells within each lymphocyte subset.

diversity of the repertoire improved markedly at 9 months, except in patient 3, who showed a sustained increase in V β 6⁺ CD8⁺ T cells.

CDR3 size distribution

Representative profiles of CDR3 size distributions from patients 3 and 4 are shown in Fig. 2. One month after transplantation, the CDR3 size distributions showed an almost normal pattern for both the CD4⁺ and CD8⁺ T cell subsets. In particular, CD4⁺ T cells from patient 3 showed completely normal patterns of CDR3 size distribution throughout the observation period. Although V β 9⁺ CD4⁺ and V β 13.2⁺ CD4⁺ T cells from patient 4 showed somewhat limited diversity at 1 and 4 months post-HSCT, the patterns had improved

significantly by 9 months. In marked contrast to CD4⁺ T cells, CDR3 distributions within CD8⁺ T cells were extremely skewed at 4 months in both patients, but the skewing of the CDR3 size distribution for CD8⁺ T cells also improved significantly at 9 months. Patients 1 and 2 showed essentially similar patterns of changes in CDR3 size distributions.

Complexity score (CS) for the TCRV β CDR3 size distribution

The diversities of CDR3 size distributions were expressed as a complexity score (CS) and plotted for each TCR V β repertoire (Fig. 3). Sequential changes of CS for all patients are shown in Fig. 3. CS for CD4⁺ T cells reached an almost normal level 1 month after HSCT and the values remained

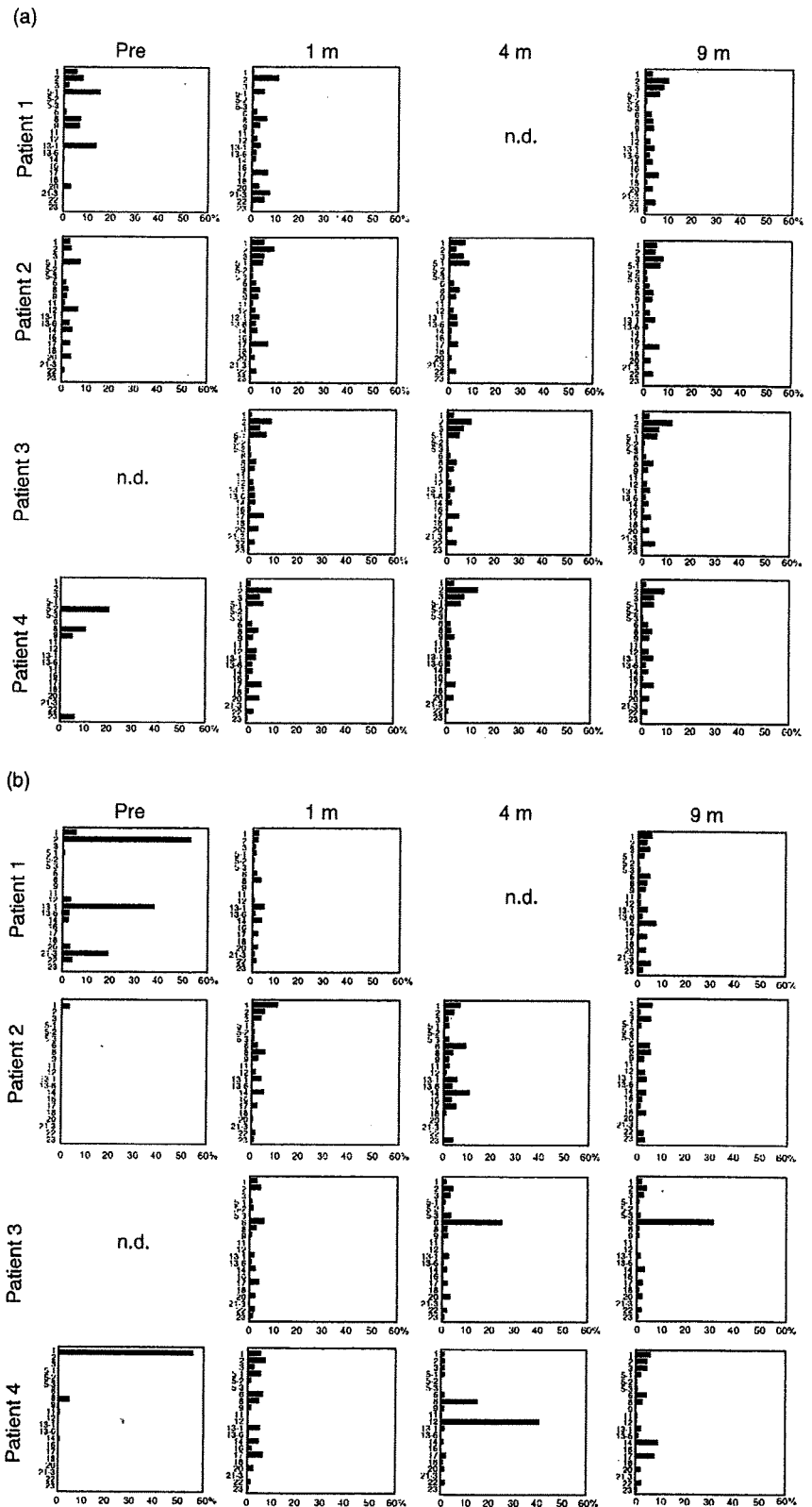


Fig. 1. Sequential changes in T cell receptor (TCR) V β repertoire distribution. TCR V β repertoire distributions for CD4⁺ T cells (a) and CD8⁺ T cells (b) were determined by a flow cytometry.

high in patients 1–3. In patient 4, in whom *Mycobacterium avium* complex infection persisted for several months, the CS improved after HSCT but remained low at 1 month. However, the CS increased progressively thereafter and

reached a normal level at 9 months. Patient 2 experienced grade IV GVHD, and significant proportions of the V β repertoire showed a low CS or were undetectable at 4 and 9 months post-HSCT. The CS for CD8⁺ T cells improved

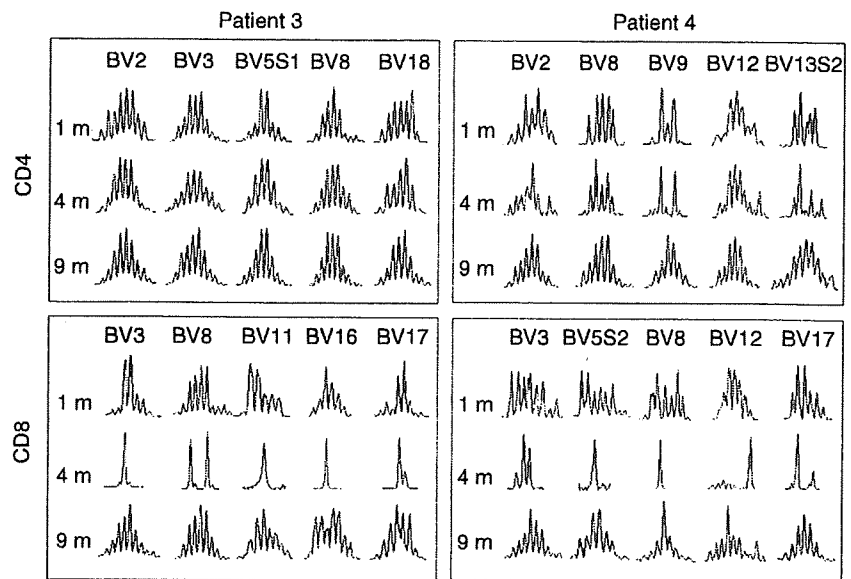


Fig. 2. Representative profiles of CDR3 size distribution after haematopoietic stem cell transplantation (HSCT). Representative profiles of the CDR3 size distributions from patients 3 and 4 are shown at 1, 4 and 9 months after HSCT. Five independent V β repertoires were chosen as representative profiles for CD4 $^{+}$ T and CD8 $^{+}$ T cells.

markedly at 1 month in all patients; however, in contrast to CD4 $^{+}$ T cells, the CS for CD8 $^{+}$ T cells decreased significantly after 4 months, but then increased again at 9 months. Recovery of the CS for CD8 $^{+}$ T cells was delayed in patient 2.

Combined qualitative and quantitative analysis of TCR repertoires

An improved visual representation was obtained by combining the results of TCR V β repertoire distributions and CDR3 size distributions, and this allowed analysis of sequential changes in TCR diversities. In marked contrast to pre-HSCT data, which showed extremely limited TCR diversity, as highlighted by the scarcity of columns and lack of Gaussian distributions for each V β repertoire, the TCR diversity of CD4 $^{+}$ T cells improved significantly at 1 month post-HSCT in all patients and the diversities were maintained until 9 months

after transplantation (Fig. 4a). However, the patterns in patient 2 showed slightly skewed distributions at 4 and 9 months. A similar improvement in TCR diversity was observed in CD8 $^{+}$ T cells after 1 month, but TCR diversity became markedly limited at 4 months, with a significant loss of detectable columns and a predominance of certain columns. These patterns improved at 9 months in all cases, but recovery was incomplete in patient 2 (Fig. 4b).

DNA sequence analysis in the TCRV β CDR3 region

DNA sequences in the CD4 $^{+}$ TCRV β 2 CDR3 region were analysed in patients 3 and 4. This particular TCRV β 2 repertoire was chosen for analysis because of its high frequency within CD4 $^{+}$ T cells, which enabled relatively easy acquisition of a large numbers of clones. In patient 3, eight of 56 clones obtained after 1 month were also detected in clones obtained

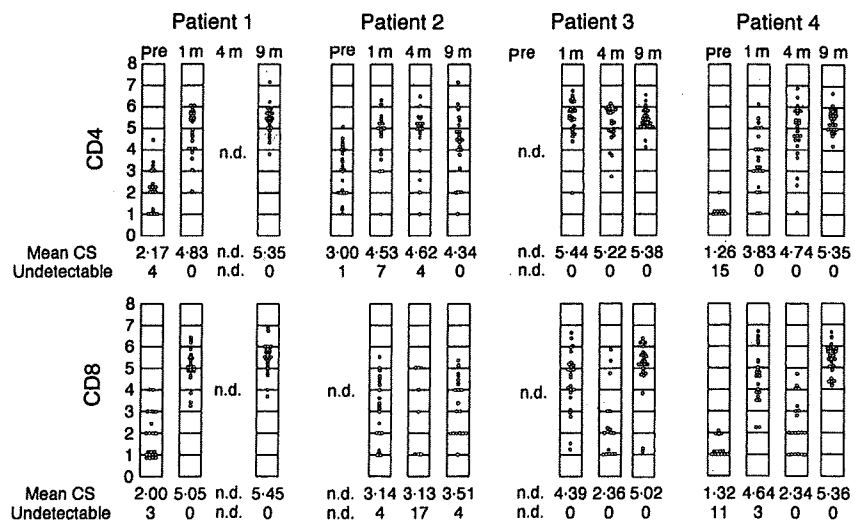


Fig. 3. Sequential changes in CDR3 complexity scores (CS). Complexity scores for each T cell receptor V β repertoire are shown. Each circle represents the CS for each repertoire; n.d.: not determined.

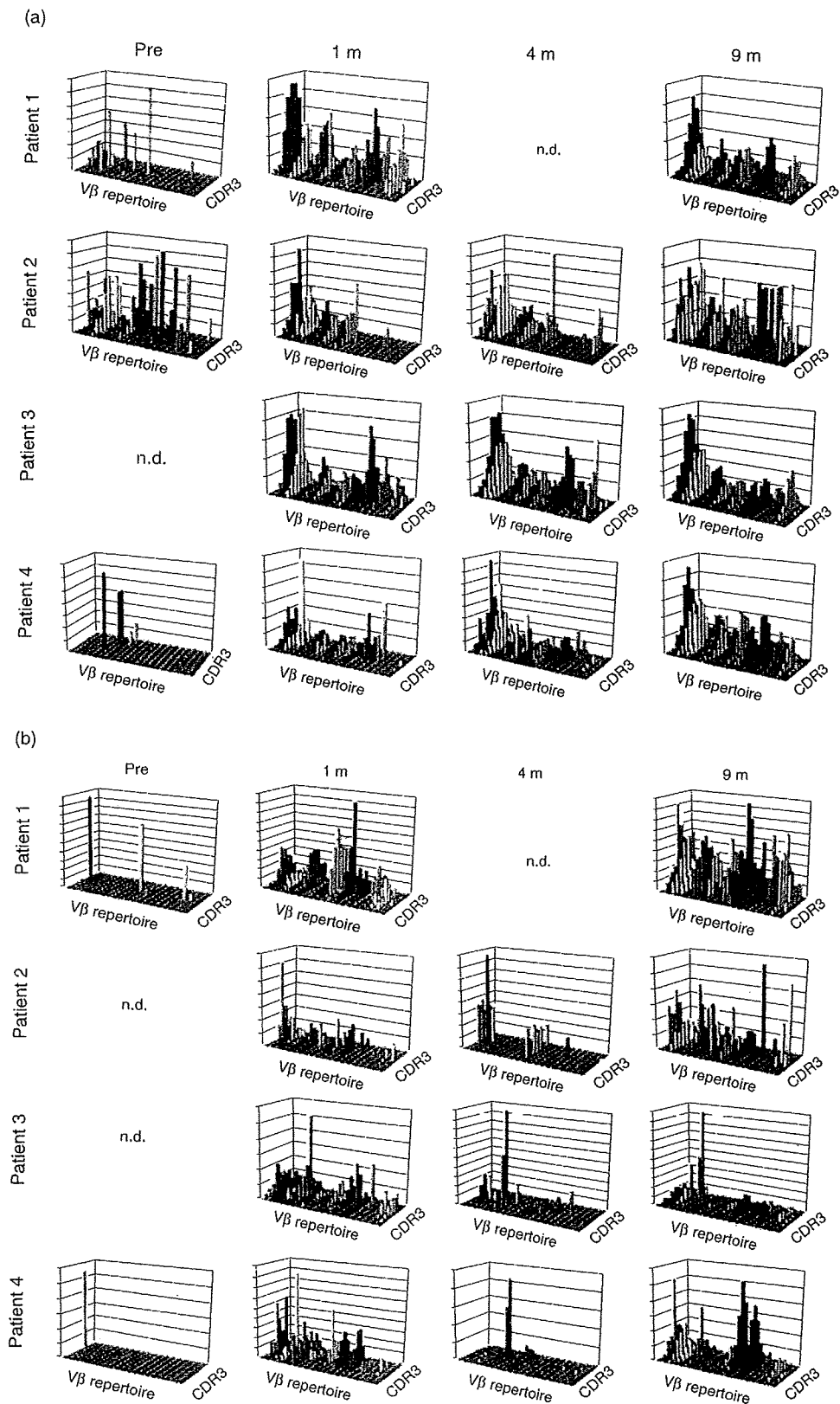


Fig. 4. Simultaneous combined display of T cell receptor (TCR) V β repertoire distribution and CDR3 size distribution. Data from qualitative analysis (CDR3 sizes) and quantitative analysis (TCR V β repertoires) are displayed visually as graphic landscape columns for CD4⁺ T cells (a) and CD8⁺ T cells (b). Identical V β repertoires are shown in the same colour. Values on the vertical axis are relative and do not represent absolute numbers; n.d.: not determined.

(a)

Donor (Father's BM)				1 m				4 m				9 m			
BV	N-D-N	BJ	Frequency	BV	N-D-N	BJ	Frequency	BV	N-D-N	BJ	Frequency	BV	N-D-N	BJ	Frequency
CSA	RALTGLAGEDFYNEQF	FGPG	1/137	CSA	SPYSYLAVKMETQY	FGPG	1/56	CSA	PTHFIRPVSAYHQY	FGPG	1/78	CSA	RDGSGFLSSYNSPLH	FGNG	1/53
CSA	SGNRVGGSGANVLT	FGAG	1/137	CSA	RGQTPGRSTDTQY	FGPG	2/56	CSA	ASKLTYGRAHEQF	FGPG	1/78	CSA	RVWDRAPSGANVLT	FGAG	1/53
CSA	VFFPKTNTGELF	FGEG	1/137	CSA	SSYGNRRDYEOF	FGPG	1/56	CSA	SGAGGAYSNOQPH	FGDG	1/78	CSA	REDGRSRYTGELF	FGEG	1/53
CSA	RDSLAGGSGELF	FGEG	3/137	CSA	AGADYYIEQIFW	FGPG	1/56	CSA	KTYKQSSSYEQY	FGPG	1/78	CSA	RYTSGRAVPDTQY	FGPG	1/53
CSA	YQAGTYNEQF	FGPG	2/137	CSA	RRGSSGTYNEQF	FGPG	1/56	CSA	SGTSGRVKYEQY	FGPG	2/78	CSA	RTPREGLNYGYT	FGSG	2/53
CSA	YQAGTYNEQF	FGPG	1/137	CSA	SPFLGGIDNEQF	FGPG	1/56	CSA	GDSSRATYNEQF	FGPG	1/78	CSA	KRAGLNTGELF	FGEG	1/53
CSA	RDASRQTDQY	FGPG	3/137	CSA	KVVGTYNNEQF	FGPG	1/56	CSA	FCRDGRYGYT	FGPG	1/78	CSA	RPGLAGPYGOY	FGPG	1/53
CSA	YQAGTYNEQF	FGPG	1/137	CSA	LDVAGGYNEQF	FGPG	1/56	CSA	RDPGGRYNEQF	FGPG	1/78	CSA	FOREWAYEQY	FGPG	1/53
CSA	YQAGTYNEQF	FGPG	2/137	CSA	RDPGGYSYEQY	FGPG	2/56	CSA	YGLAGTYNEQF	FGPG	1/78	CSA	RATGWAEQY	FGPG	2/53
CSA	PTSGRYNEQF	FGPG	3/137	CSA	MGSSNTEAF	FGQG	1/56	CSA	ALAGVDEQY	FGPG	1/78	CSA	VTSORLYEQY	FGPG	1/53
CSA	SAEDHTDTQY	FGPG	3/137	CSA	KGTGKNEQF	FGPG	2/56	CSA	PGAGANEKLF	FGSG	1/78	CSA	ERQLOEQY	FGPG	1/53
CSA	SSGTEETQY	FGPG	3/137	CSA	RVVGRGYEQY	FGPG	3/56	CSA	SGTGFGGYT	FGSG	1/78	CSA	SAGEYNEQF	FGPG	2/53
CSA	TDSNTGELF	FGEG	3/137	CSA	EGPNTGELF	FGEG	2/56	CSA	ATGMRNEPF	FGPG	1/78	CSA	TDSNTGELF	FGEG	1/53
CSA	TQSTDTQY	FGPG	3/137	CSA	TDSNTGELF	FGEG	3/56	CSA	IPNGGDTQY	FGPG	1/78	CSA	AGNTGQQF	FGPG	1/53
CSA	ITRDYGYA	FGSG	3/137	CSA	TSPGEDTQY	FGPG	1/56	CSA	PETDGYEQY	FGPG	1/78	CSA	RAPTGELF	FGEG	1/53
CSA	SYRYEKL	FGSG	2/137	CSV	PRVVVAEAF	FGQG	2/56	CSA	GLAADTQY	FGSG	1/78	CSA	TPKGNQY	FGAG	1/53
CSA	TQFYEQY	FGPG	1/137	CSA	PPRRYEQY	FGPG	1/56	CSA	SYRYEKL	FGSG	1/78	CSA	DRESMOY	FGPG	1/53
CSA	TRAGYEQY	FGPG	3/137	CSA	TQFYEQY	FGPG	2/56	CSA	RDPTGELF	FGEG	1/78	CSA	RELDEQF	FGPG	1/53
CSA	IDLYTQY	FGPG	1/137	CSA	TRPGYEQY	FGPG	1/56	CSA	EGGATEAF	FGQG	1/78	CSA	SLRGA	FGQG	1/53
Others			92/137	CSA	TSTAORY	FGPG	2/56	CSA	RGQNTIY	FGEG	1/78	Others			30/53
				Others			25/56	Others			5/78				

(b)

Donor (cord blood)				1 m			
BV	N-D-N	BJ	Frequency	BV	N-D-N	BJ	Frequency
CSA	YQQRDRVFDTGELF	FGEG	2/124	CSA	SGGHSTAGDSNTGELF	FGEG	1/56
CSA	KDRLAGKRFHEQY	FGPG	2/124	CSA	SPYSYLAVKMETQY	FGPG	1/56
CSA	RTGLAFNSDTQY	FGPG	1/124	CSA	RDGGRKSTGELF	FGEG	3/56
CSA	RVEEQATRDQY	FGEG	2/124	CSA	KVTGGLSYGYT	FGSG	1/56
CSA	MGLAGSSYEQY	FGPG	1/124	CSA	LRAGGSNOQPH	FGDG	1/56
CSA	RDLRHRQETQY	FGPG	1/124	CSA	PPLAGPYNEQF	FGPG	2/56
CSA	RDQRTSAYTQY	FGEG	1/124	CSA	RDPSSGGDNEQF	FGPG	1/56
CSA	RDRIGGTDQY	FGPG	1/124	CSA	RDGTNNSPLH	FGKG	1/56
CSA	AGTSNVDTQY	FGPG	6/124	CSA	RGTSGYNEQF	FGPG	2/56
CSA	DTSRGAWEQY	FGQG	2/124	CSA	RLAGGSNEQF	FGQG	2/56
CSA	GSGGAQETQY	FGPG	1/124	CSA	RSGTSKNIQY	FGAG	2/56
CSA	GTSGSYNEQF	FGPG	2/124	CSA	RWGDSYNGQF	FGPG	2/56
CSA	YSGSRTDTQY	FGPG	2/124	CSA	PGQLENEQF	FGPG	1/56
CSV	DGRPMNTEAF	FGQG	2/124	CSA	RGGRNQPH	FGDG	4/56
CSA	DSRGFYEQY	FGPG	1/124	CSA	SSGTEERQY	FGPG	5/56
CSA	IMGNOFNQY	FGPG	2/124	CSA	SSGVTGELF	FGEG	3/56
CSA	PLAGGHEQF	FGPG	2/124	CSA	TDSNTGELF	FGEG	1/56
CSA	RAGEDYGYT	FGSG	1/124	CSA	RDTPNIQY	FGPG	1/56
CSA	TSGRYNEQF	FGPG	1/124	CSA	SGRGSTQY	FGPG	1/56
CSA	YNRENYGYT	FGSG	2/124	CSA	SGTGYEQY	FGPG	1/56
Others			89/124	Others			20/56

Fig. 5. DNA sequence analysis in the CDR3 region. Polymerase chain reaction products of T cell receptor Vβ2 of CD4+ T cells were subcloned and the CDR3 nucleotide sequences were determined. Amino acid sequences deduced from the nucleotide sequences are shown for data obtained from donor blood, and from blood collected 1 month, 4 months and 9 months post-haematopoietic stem cell transplantation (HSCT) for patient 3 (a). Similarly, data from donor blood and for 1 month post-HSCT are shown for patient 4 (b). Identical clones are highlighted with corresponding colours in (a).

from the donor, his father (Fig. 5a). Among 137 TCRVβ2 clones from the donor, 14 shared CDR3 sequences with clones obtained from the recipient at 1 month post-HSCT. Similarly, three of 78 and one of 53 clones obtained from the recipient at 4 and 9 months, respectively, were identical to clones derived from the donor. In contrast, none of the TCRVβ2 clones obtained from the CBSCT donor blood had identical sequences to clones obtained from patient 4 at 1 month post-HSCT (Fig. 5b).

Discussion

Early reconstitution of the immune system is critical for the success of HSCT and for minimization of morbidity and mortality in SCID patients. Most transplantation-related complications, including herpes group virus infections, GVHD and thrombotic microangiopathy, occur very early after the procedure [24–26]. Recent findings indicate that at least some of these events are causally attributable to

immune dysfunction or delayed reconstitution of a normal immune system [27–29]. Impaired expansion of a diverse T cell repertoire may lead to severe infections, and a lack of regulatory T cells may be responsible for accelerated GVHD.

T cell reconstitution after HSCT occurs through two distinct mechanisms [7,8]: the thymus-dependent pathway of T cell reconstitution generally requires months after HSCT in SCID patients because the increase in naive T cells requires normalization of the size and function of the thymus [7,9–11]; in contrast, the thymus-independent pathway is dependent only on transient expansion of donor-derived mature T cells. Although T cell depletion has been used for HSCT to prevent GVHD in past procedures, an increasing number of reports indicate the benefits of T cell repletion, rather than depletion [8,30,31].

There are several pieces of evidence for early expansion of donor-derived mature T cells. First, the appearance of thymus-derived T cell clones in the peripheral blood is very unlikely within 1 month [7,9–11]; although immune reconstitution is reported to be fast following HSCT in infancy, it still takes 5–6 months for emergence of a sizeable number of CD45RO⁻ naive T cells with high T cell receptor excision circle (TREC) values. Secondly, most early T cells express a CD45RO⁺ memory phenotype, whereas *de novo* expansion of thymus-derived T cells clones presumably gives CD45RO⁻ cells [7–9]. Thirdly, microsatellite polymorphism analysis shows that early expanding T cells are mainly of donor origin and do not reflect expansion of residual recipient T cells [16,17]. These findings are highly suggestive of early, transient expansion of donor-derived T cells, regardless of their functional relevance. However, analysis of diversity in the early expanding T cell population has not been performed in detail, and there has been no direct evidence at a clonotypic level to show that clones within the circulation of the recipient are derived from mature T cells from the donor blood.

In this study, we chose patients with mutations in *RAG1/RAG2* or *Artemis* genes, because the SCID mutations, including *RAG1/RAG2*, *Artemis* and *IL2RG* gene mutations, result in similar thymus pathology and impaired output of functional T cells [32,33]. Our data show that early expansion of T cells with relatively high diversity does occur in the very early period after HSCT. These dynamic changes of TCR diversity were not accounted for fully by examination of the TCR V β repertoire distribution only, and the CDR3 size distribution analysis was superior for detection of the oligoclonality of the T cell population within a given V β repertoire. Furthermore, simultaneous display of these two parameters indicated clearly the transient nature of the TCR diversity, both quantitatively and qualitatively. The reason why TCR diversities for CD8⁺ T cells were reduced at 4 months is unclear; however, our data suggest that early expanding T cell populations are short-lived and disappear quickly from the circulation, to be slowly replaced subsequently by a thymus-derived *de novo* T cell population [7,16]. Although the thymus-derived T cells have high TCR

diversity, the absolute number of these T cells is still small at 4 months post-HSCT. Infections and alloantigen stimulation might have affected TCR diversities, as the skewing was more prominent in patients 2 and 4, who had severe GVHD and *M. avium* complex infection, respectively.

We showed further that the early expanding T cells are derived from mature T cells of donor origin. Although CDR3 nucleotide sequences were compared for only a limited number of clones, a markedly high fraction of clones shared identical sequences in patient 3. The progressive decline of the fraction of shared clones indicates that the early expanding peripheral T cells are replaced rapidly by thymus-derived *de novo* T cell clones. Because we analysed only a fraction of a vast number of clones belonging to each TCR V β family, it is statistically unlikely that identical clones would be found within the donor and recipient T cells without an extremely high overlap in clones between donor T cells and the patient's CD4⁺ T cells at 1 month post-HSCT. Presumably the adult CD4⁺ T cells have much less diversity than cord blood CD4⁺ T cells, and this permitted detection of overlapping clones in this study. In contrast, cord blood contains diverse clones of both CD4⁺ and CD8⁺ T cells; quantitatively, this is reflected in the large proportion of CD45RO⁻ naive T cells and high TREC values [13,34].

Considering that the present study was performed in only four cases with heterogeneous clinical characteristics, we should be cautious to draw any definitive conclusion. Nevertheless, the data shown here suggest the pivotal roles played by early expanding peripheral T cells. The functional significance of the early, transient expansion of donor-derived mature T cells is multifold. First, it may offer surrogate, but effective, protective immunity during the early post-HSCT period until potent immune function is reconstituted fully. Secondly, it may prevent adverse reactions to HSCT by providing regulatory functions to control excessive killer and inflammatory reactions evoked by allogeneic stimuli [35,36]; effective induction of immune tolerance may be dependent upon this function of peripheral T cells. Thirdly, our results may offer a rationale for manipulation of donor-derived mature T cells before infusion into the recipient, thereby promoting their beneficial effects, but reducing adverse functions [35,37,38]. Further detailed analyses of the nature of the early expanding T cells and techniques for *in vitro* manipulation of this potentially valuable population of donor T cells are mandatory for future improvement of HSCT.

Acknowledgements

We thank Ms Harumi Matsukawa and Ms Mika Tamamura for their excellent technical assistance. This work was supported by a Grant-in-Aid for Scientific Research from the Ministry of Education, Culture, Sports, Science and Technology of Japan; and a grant from the Ministry of Health, Labour, and Welfare of Japan, Tokyo.

References

- 1 Auletta JJ, Lazarus HM. Immune restoration following hematopoietic stem cell transplantation: an evolving target. *Bone Marrow Transplant* 2005; **35**:835–57.
- 2 Isaacs JD, Thiel A. Stem cell transplantation for autoimmune disorders. *Immune reconstitution. Best Pract Res Clin Hematol* 2004; **17**:345–58.
- 3 Nash RA. Allogeneic HSCT for autoimmune diseases: conventional conditioning regimens. *Bone Marrow Transplant* 2003; **32** (Suppl. 1):S77–80.
- 4 Buckley RH, Schiff SE, Schiff RI *et al.* Hematopoietic stem-cell transplantation for the treatment of severe combined immunodeficiency. *N Engl J Med* 1999; **340**:508–16.
- 5 Slatter MA, Gennery AR. Umbilical cord stem cell transplantation for primary immunodeficiencies. *Exp Opin Biol Ther* 2006; **6**:555–65.
- 6 Grunebaum E, Mazzolari E, Porta F *et al.* Bone marrow transplantation for severe combined immunodeficiency. *JAMA* 2006; **295**:508–18.
- 7 Müller SM, Kohn T, Schulz AS, Debatin K-M, Friedrich W. Similar pattern of thymic-dependent T-cell reconstitution in infants with severe combined immunodeficiency after human leukocyte antigen (HLA)-identical and HLA-nonidentical stem cell transplantation. *Blood* 2000; **96**:4344–9.
- 8 Lewin SR, Heller G, Zhang L *et al.* Direct evidence for new T-cell generation by patients after either T-cell-depleted or unmodified allogeneic hematopoietic stem cell transplantations. *Blood* 2002; **100**:2235–42.
- 9 Patel DD, Gooding ME, Parratt RE, Curtis KM, Haynes BF, Buckley RH. Thymic function after hematopoietic stem-cell transplantation for the treatment of severe combined immunodeficiency. *N Engl J Med* 2000; **342**:1325–32.
- 10 Myers LA, Patel DD, Puck JM, Buckley RH. Hematopoietic stem cell transplantation for severe combined immunodeficiency in the neonatal period leads to superior thymic output and improved survival. *Blood* 2002; **99**:872–8.
- 11 Sarzotti N, Patel D, Li X *et al.* T cell repertoire development in humans with SCID after nonablative allogeneic marrow transplantation. *J Immunol* 2003; **170**:2711–8.
- 12 Roux E, Dumont-Girard F, Starobinski M *et al.* Recovery of immune activity after T-cell-depleted bone marrow transplantation depends on thymic activity. *Blood* 2000; **96**:2299–303.
- 13 Chen X, Barfield R, Benaim E *et al.* Prediction of T-cell reconstitution by assessment of T-cell receptor excision circle before allogeneic hematopoietic stem cell transplantation in pediatric patients. *Blood* 2005; **105**:886–93.
- 14 Borghans JA, Bredius RG, Hazenberg MD *et al.* Early determinants of long-term T-cell reconstitution after hematopoietic stem cell transplantation for severe combined immunodeficiency. *Blood* 2006; **108**:763–9.
- 15 van Leeuwen JEM, van Tol MJD, Joosten AM *et al.* Relationship between patterns of engraftment in peripheral blood and immune reconstitution after allogeneic bone marrow transplantation for (severe) combined immunodeficiency. *Blood* 1994; **84**:3936–47.
- 16 Roux E, Helg C, Dumont-Girard F, Chapuis B, Jeannot M, Roosnek E. Analysis of T-cell repopulation after allogeneic bone marrow transplantation: significant differences between recipients of T-cell depleted and unmanipulated grafts. *Blood* 1996; **87**:3984–92.
- 17 Wu CJ, Chillemi A, Alyea EP *et al.* Reconstitution of T-cell receptor repertoire diversity following T-cell depleted allogeneic bone marrow transplantation is related to hematopoietic chimerism. *Blood* 2000; **95**:352–9.
- 18 Wada T, Toma T, Okamoto H *et al.* Oligoclonal expansion of T lymphocytes with multiple second-site mutations leads to Omenn syndrome in a patient with RAG1-deficient severe combined immunodeficiency. *Blood* 2005; **106**:2099–101.
- 19 Mizuno K, Toma T, Tsukiji H *et al.* Selective expansion of CD16^{high} CCR2⁻ subpopulation of circulating monocytes with preferential production of haem oxygenase (HO)-1 in response to acute inflammation. *Clin Exp Immunol* 2005; **49**:1030–43.
- 20 Mizuno K, Yachie A, Nagaoki S *et al.* Oligoclonal expansion of circulating and tissue-infiltrating CD8⁺ T cells with killer/effector phenotypes in juvenile dermatomyositis syndrome. *Clin Exp Immunol* 2004; **137**:187–94.
- 21 Konno A, Okada K, Mizuno K *et al.* CD8 $\alpha\alpha$ memory effector T cells descend directly from clonally expanded CD8 α^+ β^{high} TCR $\alpha\beta$ T cells *in vivo*. *Blood* 2002; **100**:4090–7.
- 22 Wada T, Schuman SH, Garabedian EK, Yachie A, Candotti F. Analysis of T-cell repertoire diversity in Wiskott-Aldrich syndrome. *Blood* 2005; **106**:3895–7.
- 23 Yawalkar N, Ferenczi Jones DA *et al.* Profound loss of T-cell receptor repertoire complexity in cutaneous T-cell lymphoma. *Blood* 2003; **102**:4059–66.
- 24 Patel SR, Ridwan RU, Ortin M. Cytomegalovirus reactivation in pediatric hemopoietic progenitors transplant: a retrospective study on the risk factors and the efficacy of treatment. *J Pediatr Hematol Oncol* 2005; **27**:411–5.
- 25 Shimoni A, Yashurun M, Hardan I, Avigdor A, Ben-Bassat I, Nagler A. Thrombotic microangiopathy after allogeneic stem cell transplantation in the era of reduced-intensity conditioning: the incidence is not reduced. *Biol Blood Marrow Transplant* 2004; **10**:484–93.
- 26 Antin JH, Deeg HJ. Clinical spectrum of acute graft-vs.-host disease. In: Ferrara JLM, Cooke KR, Deeg HJ, eds. *Graft-vs.-host disease*. New York: Marcel Dekker, 2005:369–81.
- 27 Liu C, He M, Rooney B, Kepler TB, Chao NJ. Longitudinal analysis of T-cell receptor variable β chain repertoire in patients with acute graft-versus-host disease after allogeneic stem cell transplantation. *Biol Blood Marrow Transplant* 2006; **12**:335–45.
- 28 Zorn E. CD4⁺ CD25⁺ regulatory T cells in human hematopoietic cell transplantation. *Semin Cancer Biol* 2006; **16**:150–9.
- 29 Barrett J. Improving outcome of allogeneic stem cell transplantation by immunomodulation of the early post-transplant environment. *Curr Opin Immunol* 2006; **18**:592–8.
- 30 Elmaagacli AH, Peceny R, Steckel N *et al.* Outcome of transplantation of highly purified peripheral blood CD34⁺ cells with T-cell add-back compared with unmanipulated bone marrow or peripheral blood stem cells from HLA-identical sibling donors in patients with first chronic myeloid leukemia. *Blood* 2003; **101**:446–53.
- 31 Bhattacharya A, Slatter MA, Chapman CE *et al.* Single centre experience of umbilical cord stem cell transplantation for primary immunodeficiency. *Bone Marrow Transplant* 2005; **36**:295–9.
- 32 Cavadini P, Vermi W, Facchetti F *et al.* AIRE deficiency in thymus of 2 patients with Omenn syndrome. *J Clin Invest* 2005; **115**:728–32.
- 33 Mostoslavsky G, Fabian AJ, Rooney S, Alt FW, Mulligan RC. Complete correction of murine Artemis immunodeficiency by lentiviral vector-mediated gene transfer. *Proc Natl Acad Sci USA* 2006; **103**:16406–11.

H. Okamoto *et al.*

- 34 McFarland RD, Douek DC, Koup RA, Picker LJ. Identification of a human recent thymic emigrant phenotype. *Proc Natl Acad Sci USA* 2000; **97**:4215–20.
- 35 Hess AD. Modulation of graft-versus-host disease: role of regulatory T lymphocytes. *Biol Blood Marrow Transplant* 2006; **12**:13–22.
- 36 Rezvani K, Mielke S, Ahmadzadeh M *et al.* High donor *FOXP3*-positive regulatory T-cell (T_{reg}) content is associated with a low risk of GVHD following HLA-matched allogeneic SCT. *Blood* 2006; **108**:1291–7.
- 37 Barber LD, Madrigal JA. Exploiting beneficial alloreactive T cells. *Vox Sang* 2006; **91**:20–7.
- 38 Karim M, Feng G, Wood KJ, Bushell AR. CD25⁺ CD4⁺ regulatory T cells generated by exposure to a model protein antigen prevent allograft rejection: antigen-specific reactivation *in vivo* is critical for bystander regulation. *Blood* 2005; **105**:4871–7.

Original article

Interleukin-6 attenuates hyperthermia-induced seizures in developing rats

Mitsumasa Fukuda ^{a,*}, Takehiko Morimoto ^c, Yuka Suzuki ^{a,b},
Chiya Shinonaga ^a, Yasushi Ishida ^a

^a Department of Pediatrics, Ehime University Graduate School of Medicine, Shitsukawa, Toon, Ehime 791-0295, Japan

^b Strong Epilepsy Center, University of Rochester Medical Center, Rochester, NY, USA

^c Ehime Disabled Children's Hospital, Matsuyama, Ehime, Japan

Received 30 August 2006; received in revised form 25 April 2007; accepted 27 April 2007

Abstract

Previous studies indicated that several cytokines influenced the seizure propensity in convulsive disorders and were the cause of encephalopathies in childhood. We studied the role of one inflammatory cytokine, interleukin-6 (IL-6), in hyperthermia-induced seizures in developing rats. Twenty-four male Lewis rats (23–28 days old) were divided into three groups ($n = 8$ /IL-6 (500 ng), IL-6 (50 ng), and saline control groups). We applied human recombinant IL-6 intra-nasally to developing rats 1 h before seizures induced by moist heated air (50 °C). The seizure latency was defined as the time from hyperthermia onset until the appearance of continuous seizure discharges on electroencephalography (EEG), and the seizure duration as the duration of continuous spike and wave discharges on EEG. Five of the eight rats in the IL-6 (500 ng) group, two in the IL-6 (50 ng) group, and one in the control group exhibited no seizure discharges during the 360 s heating period. In these cases, the seizure latency time was regarded as 360 s and the seizure duration time as 0 s. The median seizure latency for the IL-6 (500 ng) group, 360 s (range: 256–360), was significantly longer than that for the control one, 249 (121–360) ($P < 0.05$). The seizure duration for the IL-6 (500 ng) group, 0 s (0–20), was significantly shorter than that for the control one, 33 (0–76) ($P < 0.025$). Also, the adenosine receptor antagonist, aminophylline, prevented these effects of IL-6 on hyperthermia-induced seizures. These results indicate that IL-6 plays an anti-convulsive role through the adenosine system in hyperthermia-induced seizures, which might be relevant as to human febrile seizures.

© 2007 Elsevier B.V. All rights reserved.

Keywords: Cytokine; Interleukin-6; Hyperthermia; Febrile; Seizure; Adenosine; Aminophylline

1. Introduction

Febrile seizures (FS) and epilepsy are the most common childhood convulsive disorders. Previous studies revealed increased plasma and cerebrospinal fluid (CSF) levels of some inflammatory cytokines in patients with FS and intractable epilepsy [1–3]. Among several cytokines, interleukin-6 (IL-6) was recognized to play

an important role, because of its high plasma and CSF concentrations in patients with severe influenza-associated encephalopathy, which has been reported to be a severe central nervous system (CNS) complication of influenza and to be more frequent in Japan [4]. The problem with these clinical findings was that it could not be determined whether the increased IL-6 concentration was the result or the cause of the CNS involvement, because blood and CSF samples were usually taken after CNS symptoms had appeared.

Hyperthermia-induced seizures (HS) in experimental animals have been used to study the mechanism of FS

* Corresponding author. Tel.: +81 89 960 5320; fax: +81 89 960 5941.

E-mail address: fukudami@dokidoki.ne.jp (M. Fukuda).

[5]. Also, several studies have revealed that another inflammatory cytokine, interleukin-1 β (IL-1 β), contributes to the generation of febrile seizures in rats [6]. However, there has been no experimental study confirming the relation between IL-6 and FS. The purpose of the present study is to confirm the effect of IL-6 on the propensity of HS in developing rats.

2. Materials and methods

Twenty-four male Lewis rats (23–28 days of age) were used. They were kept with their mothers under a standard schedule of 12 h light–12 h dark, controlled temperature, and free food and water in quiet facilities during all experimental periods. After the head of a rat had been fixed to a stereotaxic holder (Narishige Co., Ltd., Tokyo, Japan), two holes were made in the skull over the right frontal and occipital cortex, and silver screw electrodes (Unique Medical Co., Ltd., Tokyo, Japan) for electroencephalography (EEG) were placed in them. These manipulations were performed under anesthesia with pentobarbital sodium (Dainippon Pharma Co., Ltd., Osaka, Japan), 30 mg/kg, and ketamine hydrochloride (Sankyo Co., Ltd., Tokyo, Japan), 50 mg/kg, intra-peritoneally. Also, cefotaxime sodium (Aventis Pharma Co., Ltd., Tokyo, Japan), 500 mg/kg, was injected to prevent bacterial infections intra-peritoneally. The rats were divided into three groups ($n = 8$ for each): control, IL-6 (50 ng/rat), and IL-6 (500 ng/rat) groups at 48 h after the surgery. Recombinant human IL-6 (Bender MedSystems, Vienna, Austria) dissolved in 0.9% saline in total volume of 20 μ l, was given intra-nasally for each rat in the IL-6 groups, because previous reports indicated intra-nasal administration was suitable for IL-6 to reach the brain and to affect seizures, and 0.9% saline was given to the control group. At 1 h after intra-nasal administration of saline or recombinant human IL-6, each rat was placed in a special plastic cage and hyperthermia-induced seizures were induced with moist warm air (50 °C), with monitoring by EEG. The seizure latency was defined as the time from hyperthermia onset until the appearance of continuous seizure discharges on EEG, and the seizure duration as the duration of continuous spike and wave discharges on EEG. In the next examination, another 24 male Lewis rats (23–28 days of age) were fitted with electrodes for EEG by the same method as described above. The rats were divided into three groups ($n = 8$ for each): control, IL-6 (500 ng), and IL-6 (500 ng) plus aminophylline groups at 72 h after the surgery. Recombinant human IL-6 (500 ng) was given intra-nasally to the IL-6 (500 ng), and IL-6 (500 ng) plus aminophylline groups, and saline to the control one. At 30 min after IL-6 administration, aminophylline (Eisai Co., Ltd., Tokyo, Japan), 5 mg/kg, was injected intra-peritoneally

for the IL-6 plus aminophylline group, and saline for the IL-6 (500 ng) and control ones. At 1 hr after intra-nasal administration of saline or recombinant human IL-6, each rat was placed in a special plastic cage and hyperthermia-induced seizures were induced with moist warm air (50 °C), with monitoring by EEG. The seizure latency and seizure duration were determined in the same way as described above. Finally, three male Lewis rats (23–28 days of age) were used for measurement of the CNS IL-6 concentration. Recombinant human IL-6 (500 ng), dissolved in 0.9% saline in total volume of 20 μ l, was given intra-nasally to these three rats. At 1 h after intra-nasal administration of IL-6, each rat was anesthetized with diethyl ether (Kanto Chemical Co., Inc., Tokyo, Japan), and its brain was removed quickly. The frontal lobes (anterior to the optic chiasma) were isolated and stored at –80 °C until the assay. Samples were weighed and homogenized in 50 mM PBS (pH 7.4). Thereafter, they were centrifuged for 15 min (5000 rpm), and the supernatants were removed and stored. IL-6 Human Easy ELISA (Amersham biosciences UK Ltd., Buckinghamshire, England) was performed to determine the level of human IL-6 in the frontal lobe. The Kruskal–Wallis test and the Bonferroni post hoc test were performed for statistical analysis.

All experimental procedures conformed to the guidelines of the Ministry of Education of Japan, and were approved by the animal experimental committee of Ehime University School of Medicine (No. TE-17-2).

3. Results

Sporadic spike and wave bursts were induced after a few minutes when rats were warmed with moist heated air (Fig. 1). Five of the eight rats in the IL-6 (500 ng) group, two of the eight in the IL-6 (50 ng) one, and one of the eight in the control one exhibited no seizure discharges during the 360 s heating period. In these cases, the seizure latency time was regarded as 360 s and the seizure duration as 0 s. The median seizure latencies for the control, IL-6 (50 ng), and IL-6 (500 ng) groups were 249 s (range: 121–360), 269 (205–360), and 360 (256–360), respectively. Thus, the seizure latency for the IL-6 (500 ng) group was significantly longer than that for the control one ($P < 0.05$) (Fig. 2a). The median seizure durations for the control, IL-6 (50 ng), and IL-6 (500 ng) groups were 33 s (range: 0–76), 20 (0–64), and 0 (0–20), respectively. Thus, the seizure duration for the IL-6 (500 ng) group was significantly shorter than that for the control one ($P < 0.025$) (Fig. 2b). In the next examination, two of the eight rats in the IL-6 (500 ng) group exhibited no seizure discharges during the 360 s heating period. The median seizure latencies for the control, IL-6 (500 ng), and IL-6

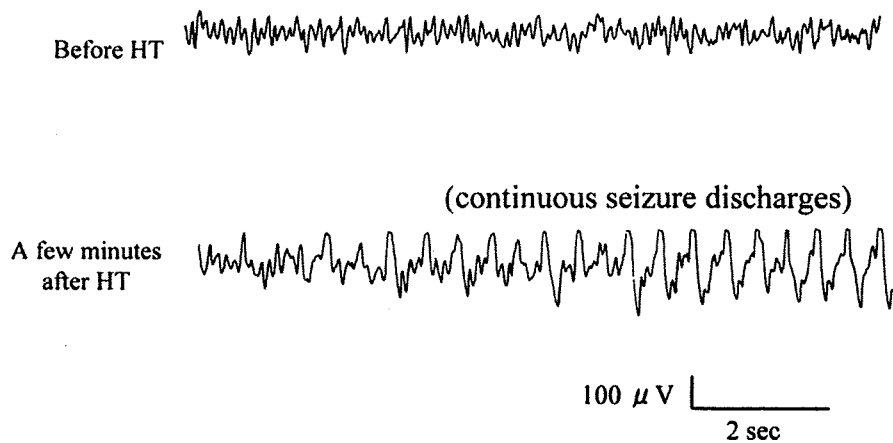


Fig. 1. EEG findings in rats. Normal 7–8 Hz background activity was recognized. Sporadic spike and wave bursts were induced a few minutes after warming with moist heated air.

(500 ng) plus aminophylline groups were 249 s (range: 179–287), 316 (243–360), and 232 (199–295), respectively. Thus, the seizure latency for the IL-6 (500 ng) group was significantly longer than that for the control one ($P < 0.025$), but there was no difference between the IL-6 (500 ng) plus aminophylline and control ones (Fig. 2c). The median seizure durations for the control, IL-6 (500 ng), and IL-6 (500 ng) plus aminophylline groups were 32 s (range: 27–51), 22 (0–37), and 41 (26–66), respectively. Thus, the seizure duration for the IL-6 (500 ng) group was significantly shorter than that for the control one ($P < 0.05$), but there was no difference between IL-6 (500 ng) plus aminophylline and control ones (Fig. 2d).

Also, the median IL-6 concentration in the brains of IL-6 (500 mg) administered rats was 50 pg/ml (range: 46–74) in the frontal lobe.

4. Discussion

Recent reports have revealed the relation between pro- or anti-inflammatory cytokines and childhood convulsive disorders. IL-1 β is one of the pro-inflammatory cytokines that play important roles in host defense responses to infection and inflammation. There have been some reports about the possible involvement of IL-1 β in FS, with respect to the plasma or cerebrospinal fluid level, IL-1 β production by peripheral blood mononuclear cells [7], and genetic polymorphic markers [8]. Regarding previous experimental findings, it has been reported that IL-1 β receptor-deficient mice are resistant to experimental FS [6], and IL-1 β suppresses the GABA_A receptor function [9]. On the other hand, there have been some reports indicating that high plasma or cerebrospinal fluid levels of IL-6 were

found in patients with influenza-associated encephalopathy and intractable convulsive disorders in childhood [3,4]. But it could not be determined whether the high IL-6 concentrations were the result or the cause of the CNS involvement, because the levels of some pro-inflammatory cytokine mRNAs, which are associated with the production of cytokines, become elevated with experimental seizures induced by electrical stimulation [10].

In the present study, recombinant human IL-6 was administered nasally, and previous studies revealed that intra-nasal administration was appropriate for several cytokines and polypeptides to bypass the blood–brain barrier [11,12]. It has been reported that the median CNS IL-6 concentration in patients with non-fulminant influenza-associated encephalopathy is 16.2 pg/ml (range: 10.2–26.9), the concentrations in fulminant ones being reported to be 855.2 and 62,250 pg/ml [13]. In the present study, the median CNS level of IL-6 in IL-6 (500 mg) administered rats was 50 pg/ml (range: 46–74), which was higher than that in non-fulminant patients, and lower than those in fulminant ones.

Based on previous experimental findings regarding the relation between IL-6 and seizure propensity, it has been reported that intra-nasal IL-6 administration increases the severity of pentylenetetrazole-induced seizures [14]. In that study, it was indicated that IL-6 increased the propensity of chemical-induced seizures in adult rats. But the relation between the propensity of HS and IL-6 in developing rats has not been reported yet. The present study revealed that intra-nasal administration of IL-6 increased the seizure threshold and shortened the seizure duration in HS. These findings indicate that IL-6 decreases the propensity of HS in developing rats. It has been reported that stimulation with IL-6 of cultured astrocytes and brain slices of the rat cortex-

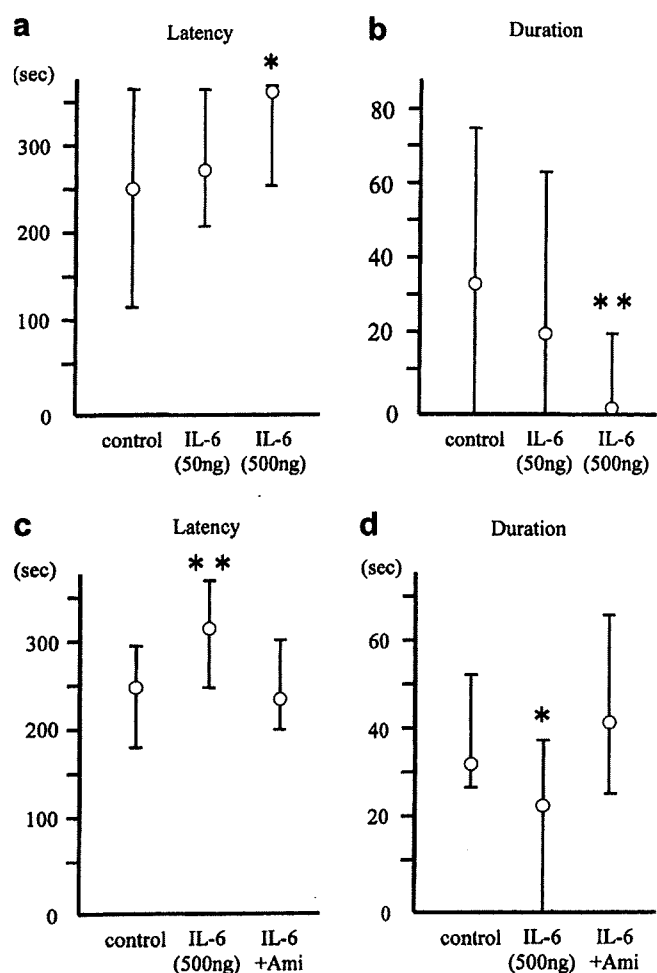


Fig. 2. * $P < 0.05$. ** $P < 0.025$. (a) Seizure latency. The data are presented as the median time and time range. The median seizure latency for the IL-6 (500 ng) group was 360 s (256–360), which was significantly longer than that for the control one 249 (121–360). (b) Seizure duration. The data are presented as the median and range. The median seizure duration for the IL-6 (500 ng) group was 0 s (range: 0–20), which was significantly shorter than that for the control one, 33 (0–76). * $P < 0.05$. ** $P < 0.025$. (c) Seizure latency. The data are presented as the median time and time range. The median seizure latency for the IL-6 (500 ng) group was 316 s (243–360), which was significantly longer than that for the control one 249 (179–287), but there was no difference between the IL-6 (500 ng) plus aminophylline group and control one. (d) Seizure duration. The median seizure duration for the IL-6 (500 ng) group was 22 s (0–37), which was significantly shorter than that for the control one 32 (27–51), but there was no difference between the IL-6 (500 ng) plus aminophylline group and control one.

induced concentration- and time-dependent upregulation of adenosine A1 receptor mRNA and adenosine A1 receptor-mediated signaling [15]. Adenosine has been said to be a powerful endogenous anti-convulsive substance in the CNS that terminates seizures [16]. Also, it has been reported that IL-6-deficient mice are a novel epileptic model, because the seizure susceptibility of these mice to some convulsants and audiogenic stimuli was greater than that of control ones [17,18]. On the other hand,

aminophylline, which is a complex of theophylline and ethylenediamine, is the adenosine receptor antagonist, and it has been reported that aminophylline exerts pro-convulsive actions in animal models [19] and humans [20]. In the present study, aminophylline abolished the anti-convulsive effect of IL-6 as to HS in developing rats. These results indicated that IL-6 might play an anti-convulsive role through the adenosine system in HS in developing rats.

Finally, we conclude that IL-6 plays an anti-convulsive role in the immature brain in hyperthermia-induced seizures, which might be relevant as to human febrile seizures.

References

- [1] Virta M, Hurme M, Helminen M. Increased plasma levels of pro- and anti-inflammatory cytokines in patients with febrile seizures. *Epilepsia* 2002;43:920–3.
- [2] Peltola J, Palmio J, Korhonen L, Suhonen J, Miettinen A, Hurme M, et al. Interleukin-6 and interleukin-1 receptor antagonist in cerebrospinal fluid from patients with recent tonic-clonic seizures. *Epilepsy Res* 2000;41:205–11.
- [3] Lehtimäki KA, Keränen T, Huhtala H, Hurme M, Ollikainen J, Honkaniemi J, et al. Regulation of IL-6 system in cerebrospinal fluid and serum compartment by seizures: the effect of seizure type and duration. *J Neuroimmunol* 2004;152:121–5.
- [4] Kawada J, Kimura H, Ito Y, Hara S, Iriyama M, Yoshikawa T, et al. Systemic cytokine responses in patients with influenza-associated encephalopathy. *J Infect Dis* 2003;188:690–8.
- [5] Morimoto T, Nagao H, Sano N, Takahashi M, Matsuda H. Electroencephalographic study of rat hyperthermic seizures. *Epilepsia* 1991;32:289–93.
- [6] Dubé C, Vezzani A, Behrens M, Bartfai T, Baram TZ. Interleukin-1 β contributes to the generation of experimental febrile seizures. *Ann Neurol* 2005;57:152–5.
- [7] Hulkkonen J, Koskikallio E, Rainesalo S, Keränen T, Hurme M, Peltola J. The balance of inhibitory and excitatory cytokines is differently regulated in vivo and in vitro among therapy resistant epilepsy patients. *Epilepsy Res* 2004;59:199–205.
- [8] Kira R, Torisu H, Takemoto M, Nomura A, Sakai Y, Sanefuji M, et al. Genetic susceptibility to simple febrile seizures: interleukin-1 β promoter polymorphisms are associated with sporadic cases. *Neurosci Lett* 2005;384:239–44.
- [9] Wang S, Cheng Q, Malik S, Yang J. Interleukin-1 β inhibits γ -aminobutyric acid type A (GABA) receptor current in cultured hippocampal neurons. *J Pharmacol Exp Ther* 2000;292:497–504.
- [10] Vezzani A, Moneta D, Ricchi C, Peregó C, De Simoni MG. Functional role of proinflammatory and anti-inflammatory cytokines in seizures. *Adv Exp Med Biol* 2004;548:123–33.
- [11] Lawrence D. Intranasal delivery could be used to administer drugs directly to the brain. *Lancet* 2002;359:1674.
- [12] Dufes C, Olivier JC, Gaillard F, Gaillard A, Couet W, Muller JM. Brain delivery of vasoactive intestinal peptide (VIP) following nasal administration to rats. *Int J Pharm* 2003;255:87–97.
- [13] Togashi T, Matsuzono Y, Narita M, Morishima T. Influenza-associated acute encephalopathy in Japanese children in 1994–2002. *Virus Res* 2004;103:75–8.
- [14] Kaluff AV, Lehtimäki KA, Ylinen A, Honkaniemi J, Peltola J. Intranasal administration of human IL-6 increases the severity of chemically induced seizures in rats. *Neurosci Lett* 2004;365:106–10.

- [15] Biber K, Lubrich B, Fiebich BL, Boddeke H, van Calker D. Interleukin-6 enhances expression of adenosine A1 receptor mRNA and signaling in cultured rat cortical astrocytes and brain slices. *Neuropsychopharmacology* 2001;24:86–96.
- [16] Dragnow M. Adenosine and seizure termination. *Ann Neurol* 1991;29:575.
- [17] Luca GD, Di Giorgio RM, Macaione S, Calpona PR, Costantino S, Di Paola ED, et al. Susceptibility to audiogenic seizures and neurotransmitter amino acid levels in different brain areas of IL-6-deficient mice. *Pharmacol Biochem Behav* 2004;78:75–81.
- [18] De Sarro G, Russo E, Ferrei G, Giuseppe B, Flocco MA, Di Paola ED, et al. Seizure susceptibility to various convulsant stimuli of knockout interleukin-6 mice. *Pharmacol Biochem Behav* 2004;77:761–6.
- [19] Ray A, Gulati K, Anand S, Vijayan VK. Pharmacological studies on mechanisms of aminophylline-induced seizures in rats. *Indian J Exp Biol* 2005;43:849–53.
- [20] Odajima Y, Nakano H, Kato T. Clinical review on patients who developed seizures during theophylline administration: relationships with seizure-predisposing factors (in Japanese). *Arerugi (Tokyo)* 2006;55:1295–303.

Silencing of *MYCN* by RNA interference induces growth inhibition, apoptotic activity and cell differentiation in a neuroblastoma cell line with *MYCN* amplification

KEIGO NARA¹, TAKESHI KUSAFUKA², AKIHIRO YONEDA¹, TAKAHARU OUE¹,
SURASAK SANGKHATHAT¹ and MASAHIRO FUKUZAWA¹

¹Department of Pediatric Surgery, Osaka University Graduate School of Medicine, Suita, Osaka 565-0871;

²Department of Pediatric Surgery, Nihon University School of Medicine, Itabashi, Tokyo 173-8610, Japan

Received November 24, 2006; Accepted January 19, 2007

Abstract. Although it has been suggested that the *MYCN* oncoprotein functions may influence tumorigenesis and patient survival in neuroblastoma, the mechanism of these functions remains unclear. To elucidate such molecular and biological mechanisms, we performed knock-down of *MYCN* expression using RNA interference (RNAi) method. *MYCN*-siRNAs (*MYCN*-siRNA) were transfected into the *MYCN*-amplified cell line NB-1. To verify the sequence specificity of the siRNA, we prepared three control groups (siRNA control group: siRNAs with no significant homology to any known sequences in human genome, mock control group: reagent and PBS, and the untransfected control group). The cells were analyzed by real-time RT-PCR, Western blotting, immunocytochemistry for gene expression. Cell proliferation activity was measured by WST-1 assay. TUNEL staining was performed to evaluate apoptosis. After the *MYCN*-siRNA transfection, the expression level of the *MYCN* mRNA was significantly reduced to 30% of those of the three control groups ($p < 0.05$). Western blotting revealed an obvious reduction in *MYCN* protein level in the *MYCN*-siRNA group. On immunocytochemistry, intensity of nuclear staining of *MYCN* was weaker in the *MYCN*-siRNA group than in the three control groups. On WST-1 viability assay, cell proliferation after the *MYCN*-siRNA transfection was significantly suppressed compared to the three control groups ($p < 0.05$). The TUNEL positive cells were frequently observed in the *MYCN*-siRNA group. Additionally, after the *MYCN*-siRNA transfection, the morphologic change which was suggestive of neuronal cell differentiation was observed and *TrkA* and *TrkC* expressions were also significantly up-regulated. Using RNAi method, the knock-down of *MYCN*

expression induced growth-inhibition, apoptotic activity and cell differentiation in *MYCN*-amplified NB-1 cell line.

Introduction

Neuroblastoma (NB), a malignant neoplasm of neural crest origin, is the most common solid extracranial tumor in children and is responsible for 15% of pediatric cancer deaths (1-3). The advent of combination of surgery, chemotherapy and radiation therapy, in addition to high dose chemotherapy with stem cell rescue has made significant improvement in terms of survival rates for advanced NBs. However, the prognosis of the advanced NBs, especially tumors with *MYCN* amplification, remains poor (4,5).

MYCN is one of *MYC* family members which are transcription factors that contain to a transcriptional activation domain and a transcriptional regulation domain (6,7). While *MYCN* expression is limited to early stages of embryonic development, the *MYC* gene is expressed in a wide variety of tissues. *MYCN* is normally located on the distal short arm of chromosome 2, but in cells with *MYCN* amplification it also maps to the double minutes or homogeneously staining regions (8). A large region from chromosome 2p24 (including the *MYCN* locus) becomes amplified, presumably because it provides some selective advantage to the cells (7).

In clinical studies *MYCN* amplification has been correlated with advanced stages of disease and rapid tumor progression (9-11). It is generally accepted that amplification of the *MYCN* oncogene is more relevant to prognosis than other prognostic factors such as chromosome 1p deletion, diploid DNA content and *TrkA* expression. In general, there is a correlation between *MYCN* copy number and expression (11,12). Furthermore, a couple of reports have suggested an association between *MYCN* overexpression and patients' prognosis (12). However, it is still controversial whether or not overexpression of *MYCN* mRNA or *MYCN* protein has prognostic significance in tumors lacking *MYCN* amplification (13-15).

In an experimental model, it was reported that transgenic mice with overexpression of *MYCN* developed NBs (16). Moreover, Manohar *et al* have shown direct evidence that *MYCN* induction in human NB cells resulted in increased *MRP1* mRNA and protein levels, which in turn was

Correspondence to: Dr Akihiro Yoneda, Department of Pediatric Surgery, Osaka University Graduate School of Medicine, 2-2 Yamadaoka, Suita, Osaka 565-0871, Japan
E-mail: yoneda@ped surg.med.osaka-u.ac.jp

Key words: *MYCN*, neuroblastoma, RNA interference